Extracting a value of the deuteron radius by reanalysis of the experimental data

Mustafa M. Mustafa
Department of Physics, Faculty of Science (Sohag), Assiut University, Sohag, Egypt

El-Shazli M. Hassan
Department of Physics, Faculty of Science (Qena), Assiut University, Qena, Egypt

Mark W. Kermode
Department of Applied Mathematics and Theoretical Physics, University of Liverpool, P.O. Box 147, Liverpool L69 3BX, United Kingdom

Elbadry M. Zahran
Department of Physics, Faculty of Science, Assiut University, Assiut, Egypt
(Received 10 February 1992)

A new value, $r_D = 1.9546 \pm 0.0021$ fm, for the rms radius of the deuteron has been extracted by reanalyzing the experimental data for the ratio $R(q^2)$ of the deuteron to proton electric form factors and for the slope of the neutron electric form factor $G_{En}(q^2)$ at $q^2 = 0$. The short-range structures in the radial deuteron wave functions found for a certain class of potentials (e.g., Kermode *et al.* and potential models presented here) cause an increase in the model values of the deuteron charge form factor $C_E(q^2)$, but have no special features in the variation of $C_E(q^2)$ with q^2. A new method for calculating $C_E(q^2)$ accurately is presented.

PACS number(s): 21.30.+y, 13.75.Cs, 21.45.+v, 21.10.Ft

I. INTRODUCTION

Several works [1–6] have been reported in the literature on extracting the root-mean-square (rms) matter radius of the deuteron r_D from the measurements of the elastic scattering of electrons by deuterons and protons. Berard *et al.* [1] found an empirical linear relation between b and r_D for deuteron potential models, where b is the slope of the neutron form factor $G_{En}(q^2)$ at $q^2 = 0$. They used their experimental data for the ratio $R(q^2) = G_{ED}/G_{Ep}$ of the deuteron to proton electric form factors in the calculations of b. The extracted value $r_D = 1.9635 \pm 0.0045$ fm corresponds to the experimental value $b = 0.0189 \pm 0.0004$ fm^{-2} given by Krohn and Ringo [7]. Akimov *et al.* [2] used their experimental data for the deuteron electric form factor $G_{ED}(q^2)$, and obtained 1.944 ± 0.028 fm for r_D. They also obtained three other values for r_D corresponding to three values of the proton radius r_p: they are $r_D = 1.947 \pm 0.029$, 1.935 ± 0.029, and 1.921 ± 0.029 fm corresponding to $r_p = 0.81 \pm 0.01$, 0.84 ± 0.01, and 0.87 ± 0.01 fm, respectively. Simon *et al.* [3] used their measurements of $R(q^2)$ and obtained $r_D = 1.9625 \pm 0.0047$ fm ($r_D = 1.9560 \pm 0.0068$ fm), by fitting their data with polynomials of order three (four).

Experimental data have been reanalyzed by Allen *et al.* [4], McTavish [5], and Klarsfeld *et al.* [6]. For the radial deuteron wave functions of a given potential model and their family of the wave functions produced by unitary transformations, Allen *et al.* [4] found a linear relation between r_D^2 and b. The experimental value $b = 0.0199 \pm 0.0003$ fm^2 given by Koester *et al.* [8] has been used to determine r_D "indirectly" from the plotted straight line. The points (r_D^2, b) have the common property that all the wave functions are similar at large values of r; hence, they have the same values of the asymptotic S-state amplitude A_S and the asymptotic ratio η. The experimental value of r_D was not obtained directly from the graph because the deuteron wave functions used did not have the correct experimental values of both A_S and η. Allen *et al.* [4] assumed that η is more accurately measured than A_S and that a small change in η is proportional to a small change in r_D^2. They obtained $r_D = 1.952 \pm 0.004$ fm which corresponds to the then experimental value [4] of η of 0.0264 ± 0.0003.

McTavish [5] used the experimental data of Berard *et al.* [1] for the ratio $R(q^2)$ to obtain the "experimental" values of the charge form factor $C_E(q^2)$. He modified Wilson's expansion [9] of $C_E(q^2)$ and used it in a one-parameter fit to obtain $r_D = 1.956 \pm 0.005$ fm.

The contribution of the asymptotic terms of the parametrized form of the radial deuteron wave functions u and w of the Paris potential [10] (but with values for A_S and η given by $A_S = 0.8800 \pm 0.0060$ fm$^{-1/2}$ which is an average of several measurements [6], and $\eta = 0.0268 \pm 0.0007$[11] has been used in the expansion of $C_E(q^2)$ in powers of q^2 by Klarsfeld *et al.* [6] to determine the higher-order moments $\langle r^{2n} \rangle$. They fitted the data of Simon *et al.* [3] and Berard *et al.* [1] and obtained $r_D = 1.953 \pm 0.003$ fm.

The aim of this work is an attempt to improve the determination of the root-mean-square (rms) radius of the

deuteron r_D from the experimentally determined electric form factor ratio $R(q^2)$ and from the slope b of the neutron electric form factor $G_{En}(q^2)$ at $q^2=0$.

II. A LOCAL POTENTIAL MODEL WITH CORRECT A_S AND η

At present there is no potential model which gives the correct experimental values of A_S and η. Approximations made by Allen *et al.* [4] are not adequate to compensate for the absence of such potential. For example, their extracted value $r_D=1.952\pm0.004$ fm may be changed to be $r_D=1.954\pm0.003$ fm if the Reid soft-core potential [12] is used in the analysis [4] or to be $r_D=1.958\pm0.003$ fm if the value extracted for r_D is to be consistent with the experimental value of A_S instead of that of η [5]. Also, in the absence of such a potential, Klarsfeld *et al.* [6] used, in their "asymptotic method" to obtain r_D, a parametrization of the radial deuteron wave functions consisting of a mixture of terms like those of the parametrizations of the radial wave functions by Paris [10], Hulthén and Sugawara [13], and Adler *et al.* [14].

We present here a potential which has the recent experimental value of $A_S=0.8838\pm0.0004$ fm$^{-1/2}$ of Stoks *et al.* [15] and $\eta=0.0273\pm0.0005$ of Borbély *et al.* [16]. The local potential has been chosen to be of Reid's hard-core type [12] and fits accurately the energy-dependent scattering parameters of Arndt *et al.* [17] (χ^2/datum 0.15) in the laboratory energy range 0–300 MeV. This potential consists of central (C), spin-orbit (LS), and tensor (T) parts:

$$V=V_C+V_{LS}\mathbf{L}\cdot\mathbf{S}+S_{12}V_T\ . \tag{2.1}$$

The functional form of each part is taken to be the sum of Yukawa potentials

$$rV_i(r)=\sum_{n=1}^{6}A_i(n)e^{-n\mu r}\ , \tag{2.2}$$

where i denotes the central and spin-orbit parts, and $\mu=0.7$ fm^{-1}. The longest-range components are determined by the one-pion exchange potential (OPEP), i.e., $A_C(1)=-14.947\,14$ MeV fm and $A_{LS}(1)=0$. The tensor part is taken to be of the form

$$V_T(r)=V_T^{(1)}(r)+V_T^{(2)}(r)\ , \tag{2.3a}$$

where

$$rV_T^{(1)}(r)=B(1)[(1+3/\mu r+3/\mu^2r^2)e^{-\mu r}-N^2(1+3/N\mu r+3/N^2\mu^2r^2)e^{-N\mu r}] \tag{2.3b}$$

and

$$rV_T^{(2)}(r)=\sum_{n=2}^{6}A_T(n)e^{-n\mu r}\ . \tag{2.3c}$$

$B(1)$ is determined by the OPEP and is equal to $-14.947\,14$ MeV fm. The value of N was taken to be $N=6$. The value 0.548 33 fm is assumed for the hard-core radius. The free parameters of this local potential are listed in Table I. Properties of the potential are given in Table II. The radial dependences of the potential and its radial deuteron wave functions are compared to those of the Reid hard-core potential [12] in Figs. 1 and 2. It is interesting to note the shape of the D-state wave function in Fig. 2. It has the form expected for a nonlocal potential, but we emphasize that this is the result for a *local* potential.

TABLE I. The free parameters of the local potential. $B(1)=-14.947\,14$ MeV fm.

n	$A_C(n)$	$A_{LS}(n)$	$A_T(n)$
1	−14.947 14	0.0	0.0
2	−1 491.328	593.9225	−421.2055
3	30 324.30	−12 351.39	6 943.784
4	−193 483.3	88 378.22	−31 696.09
5	480 649.9	−240 062.0	48 675.39
6	−405 831.0	210 874.9	−19 291.89

It is worthwhile to mention that this local potential fits the experimental value of the quadrupole moment Q of the deuteron ($Q=0.2860\pm0.0015$ fm^2 (Ref. [18]) and $Q=0.2859\pm0.0003$ fm^2 (Ref. [19])). It has been thought that the experimental value of Q is too large to be reproduced by local deuteron potentials. For example, Allen *et al.* [20] claimed that the quadrupole moment of the deuteron is almost impossible to be fitted with energy-independent potentials. Also, De Tourreil *et al.* [21] argued that no existing potential models–at that time–reproduced this high value of the deuteron quadrupole moment and that the meaning of this seemed unclear but very interesting. In a recent paper by one of us [22], two simple local potential models having $Q>0.3$ fm^2 have been given as an example for the possibility of fitting the quadrupole moment of the deuteron with local potentials.

It was difficult to fit the experimental value of the triplet scattering length $a_t=5.149\pm0.007$ fm and the triplet effective range $r_t=1.754\pm0.008$ fm by this local potential because of the correlation between r_D, A_S, and a_t [23,24].

III. EXTRACTING r_D FROM BOTH THE EXPERIMENTAL DATA ON $R(q^2)$ AND b

We used both the experimental data for $R(q^2)$ of Simon *et al.* [3], for momentum transfers $0.044\le q^2\le4$

TABLE II. Properties of the local potential of Table I.

Binding energy E_b	−2.2246 MeV
Quadrupole moment Q	0.2860 fm^2
D-state probability P_D	6.451%
Asymptotic S-state amplitude A_S	0.8838 fm$^{-1/2}$
Asymptotic D-state amplitude A_D	0.0242 fm$^{-1/2}$
The asymptotic ratio $\eta=A_D/A_S$	0.0273
rms radius r_D	1.963 fm
D_2 parameter	0.5043 fm^2
Scattering length a_t	5.396 fm
Effective range r_t	1.704 fm
Shape parameter P	0.0260

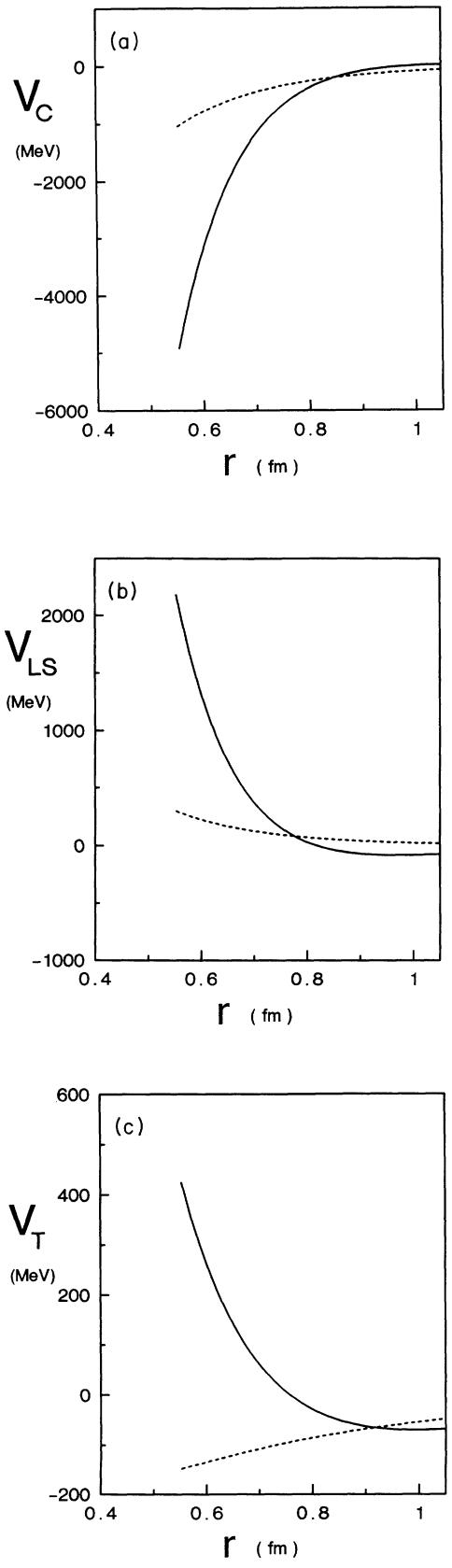

FIG. 1. (a) Central V_C, (b) spin-orbit V_{LS}, and (c) tensor V_T components of the local potential of Table I (solid lines) are compared to the Reid hard-core potential [12] (dashed lines).

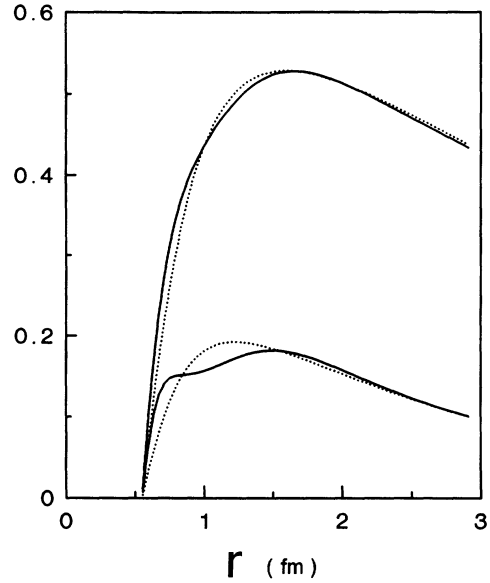

FIG. 2. The radial deuteron wave functions of the local potential of Table I (solid lines) are compared to the Reid hard-core potential [12] (dashed lines). The upper (lower) curves are the u (w) wave functions.

fm^{-2}, and the experimentally measured value $b=0.0199\pm0.0003$ fm^2 for the slope of the neutron electric form factor $G_{En}(q^2)$ at $q^2=0$ fm^{-2},

$$b=\left.\frac{dG_{En}(q^2)}{dq^2}\right|_{q^2=0}, \tag{3.1}$$

of Koester *et al.* [8] to determine r_D. The q^2 variation of the neutron electric form factor $G_{En}(q^2)$ may be obtained from

$$G_{En}(q^2)=\left[\frac{R(q^2)(1+\tau^2)^{1/2}}{C_E(q^2)}-1\right]G_{Ep}(q^2), \tag{3.2a}$$

where the proton electric form factor $G_{Ep}(q^2)$ is given by Simon *et al.* [25] as

$$G_{Ep}(q^2)=\frac{0.312}{1+q^2/6}+\frac{1.312}{1+q^2/15.02}-\frac{0.709}{1+q^2/44.08}+\frac{0.085}{1+q^2/154.2}, \tag{3.2b}$$

the deuteron charge form factor $C_E(q^2)$ is given by

$$C_E(q^2)=\int_0^\infty (u^2+w^2)j_0(qr/2)dr, \tag{3.2c}$$

$\tau=q^2/4m_p^2$, $m_p=4.761\,46$ fm^{-1} is the proton mass, and u and w are the radial deuteron wave functions. We also used the four experimental values of $R(q^2)$ at $q^2=1.55$, 2.1, 3.3, and 4.0 fm^{-2} from which Klarsfeld *et al.* [6] have subtracted the quadrupole form factor contribution (Table I of Ref. [6]).

The variation of $C_E(q^2)$ versus q^2 is first obtained by using (3.2c) for the radial deuteron wave functions of the local potential of Table I and is also obtained for each of the various radial deuteron wave functions obtained from them by applying unitary transformations of the follow-

ing form used by Kermode *et al.* [26]

$$Z=\begin{bmatrix} Z_u & 0 \\ 0 & Z_w \end{bmatrix},$$

where

$$Z_u=Z_w=Z=t(\alpha,\beta)=1-2g(s)g(s'),$$

$$g(s)=Cs(1-\beta s)e^{-\alpha s},$$

$$s=r-r_c.$$

Here, r_c in the hard-core radius, C is a normalizing constant $C=[4\alpha^5/(\alpha^2-3\alpha\beta+3\beta^2)]^{1/2}$ such that $\langle g|g\rangle=1$. The transformed deuteron wave function is given by

$$\Psi-2g(r)\int_0^\infty g(s)\Psi(s)ds,$$

where Ψ means u and w radial deuteron wave functions of the reference local potential. The parameter of the nonlocality "range" α is assumed to have the values 1.7, 2.5, 3, and 3.5 fm^{-1}. For each of these assumed values of α, the parameter of the nonlocality "strength" β is changed from $\beta=0$ fm^{-1} to $\beta=1.5$ fm^{-1} in steps of 0.1 fm^{-1}.

Then, each of these variations of $C_E(q^2)$ versus q^2 is inserted in Eq. (3.2a) to get the corresponding q^2 variation of $G_{En}(q^2)$. The model-dependent values of b are obtained by simulating each of these variations by a polynomial of order m in q^2,

$$G_{En}(q^2)=\sum_{i=1}^{i=m} b_i q^{2i}, \quad m=2,\ 3,\ 4,\ \text{and}\ 5 \qquad (3.3)$$

with $b=b_1$. For a pair (u,w) of the radial deuteron wave functions u and w, we calculate r_D^2 and four values of b corresponding to the four values of m in Eq. (3.3). Allen *et al.* [4] used only positive values of b to draw the linear r_D^2-b relation. We consider the general case here, where both negative and positive values of b are used. The variation of b versus r_D^2 for $m=3$ is shown in Fig. 3. The radial dependences of transformed deuteron wave functions having the correct value of b are shown in Fig. 4. No effect on other deuteron properties is found (other than r_D) as a result of having the same value of b, e.g., these transformed wave functions have different values for the quadrupole moment. The extracted values of r_D and the standard errors Δb close to the experimental value $b=0.0199$ fm^2 are listed in Table III. The meson exchange current (MEC) and the isobar contributions are given by Lomon [27] and have been used in the analysis

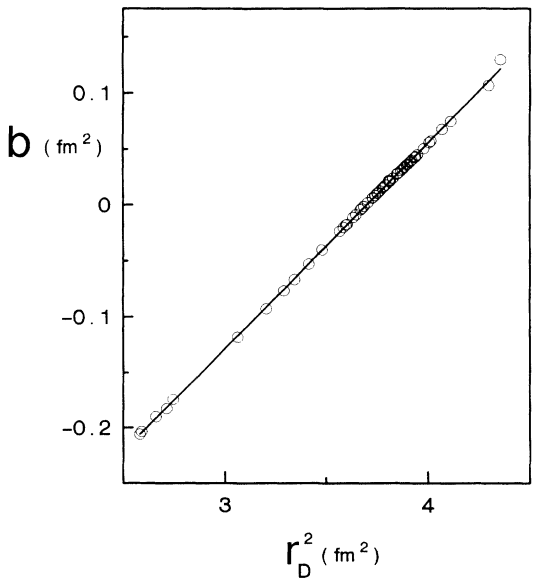

FIG. 3. The straight line representing the variation of b versus r_D^2 in the case of $m=3$. The circles represent the local potential of Table I and its phase-equivalent potentials. The error bars representing the standard errors Δb are not drawn; their lengths are shorter than the circles' radii in all cases.

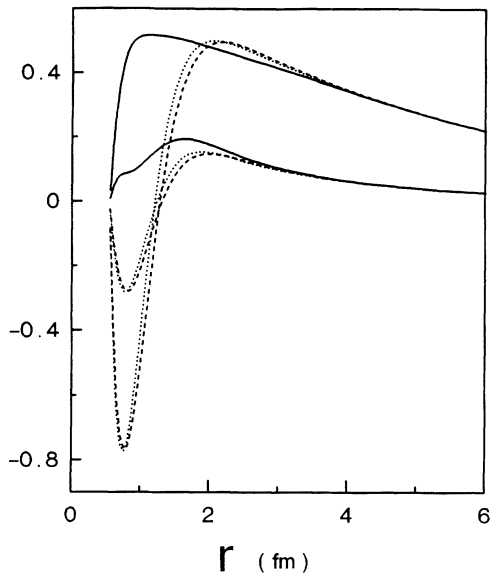

FIG. 4. Transformed radial deuteron wave functions having the correct value of b. They are obtained by using the unitary transformations with $\alpha=2.5$ fm^{-1} and $\beta=1.2$ fm^{-1} (solid lines), $\alpha=3$ fm^{-1} and $\beta=0.6$ fm^{-1} (dashed lines), and $\alpha=3.5$ fm^{-1} and $\beta=0.6$ fm^{-1} (dotted lines). The corresponding values of the deuteron quadrupole moment are 0.289, 0.280, and 0.279 fm^2, respectively. The upper (lower) curves are the u (w) wave functions.

TABLE III. The extracted values for the rms matter radius of the deuteron r_D. The q^2 variations of $G_{En}(q^2)$ (in the case of using the local potential of Table I and its phase equivalent potentials produced by unitary transformations) are simulated by polynomials of order m to obtain the corresponding values of b. The values listed for the standard error Δb are determined for values of b close to the experimental value [8] $b=0.0199$ fm^{-2} in each case. The MEC contribution [28] $\Delta r_D=0.0034\pm0.0003$ fm is taken into account.

m	Δb (fm^{-2})	r_D (fm)
2	0.0009	1.9631±0.0013
3	0.0015	1.9546±0.0021
4	0.0022	1.9549±0.0032
5	0.0038	1.9548±0.0057

of McTavish [5]. In this work, we used $\Delta r_D = 0.0034 \pm 0.0003$ fm given by Kohno [28] to take the MEC into account. It is clear from Table III that for $m \geq 3$, the extracted values of r_D, to three decimal points, are almost the same.

We ignored the contribution to the standard error Δr_D caused by the errors $\pm\Delta A_S$ and $\pm\Delta\eta$ in the experimental values of A_S and η, respectively. The determination of these contributions may be carried out by constructing local potentials having properties similar to that of the local potential of Table I, except for the values of A_S, η, and r_D. The difference between the values of A_S and η of these potentials and the value of A_S and η of the local potential of Table I should be either $\pm\Delta A_S$ with no change in η or $\pm\Delta\eta$ with no change in A_S. The required contribution of $\pm\Delta A_S$ ($\pm\Delta\eta$) to Δr_D may then be taken as the maximum difference between the values of r_D of these potentials of the first (second) case and the value of r_D of the local potential of Table I. We expect the values of these contributions to be small enough to be ignored since A_S and η change "faster" than r_D during the search procedure so that relatively large changes in A_S and η would correspond to relatively small changes in r_D. We quote

$$r_D = 1.9546 \pm 0.0021 \text{ fm} \tag{3.4}$$

corresponding to $m = 3$ as our result. This value agrees to within the quoted errors with corresponding values obtained by Allen *et al.* [4], McTavish [5] and Klarsfeld *et al.* [6]. In comparison with the case of Allen *et al.* [4], although they used a one-parameter fit to obtain b from

$$G_{En}(q^2) + 0.0036q^4 = bq^2 ,$$

their standard error for r_D is larger than the standard errors in the cases of using two-, three-, and four-parameters fits in our case (see Table III). This is because the value of r_D is "directly" extracted from the r_D^2-b graph, as we used a potential model with correct A_S and η, and also because a larger number of data pieces are involved in the fitting (16 here and 9 in their case).

Although the method used to obtain our new value of r_D involves using a potential model with correct values of A_S and η, this new value of r_D of relation (3.4) is *model independent* because the r_D^2-b lines representing different potentials are parallel and are ordered only by the values of η and A_S [4] (e.g., as η decreases and A_S increases, the lines will be shifted towards higher values of r_D^2), so that, the r_D^2-b line of any other potential model having the correct values of A_S and η would necessarily be the same as the r_D^2-b line of the local potential of Table I.

IV. A NEW METHOD FOR CALCULATING MODEL VALUES OF $C_E(q^2)$

The deuteron charge form factor $C_E(q^2)$ may be written

$$C_E(q^2) = \int_0^R (u^2 + w^2) j_0(qr/2) dr + \Delta C_E(q^2) , \tag{4.1}$$

where

$$\Delta C_E(q^2) = \int_R^\infty (u^2 + w^2) j_0(qr/2) dr . \tag{4.2}$$

For the second integral, only the asymptotic forms of the radial deuteron wave functions u and w,

$$u = A_S e^{-\gamma r} , \tag{4.3a}$$

$$w = A_D e^{-\gamma r}(1 + 3/\gamma r + 3/\gamma^2 r^2) , \tag{4.3b}$$

are required. Thus, for example, the terms in a power-series expansion of $\Delta C_E(q^2)$ can be evaluated analytically [6]. We shall present an alternative, improved approach

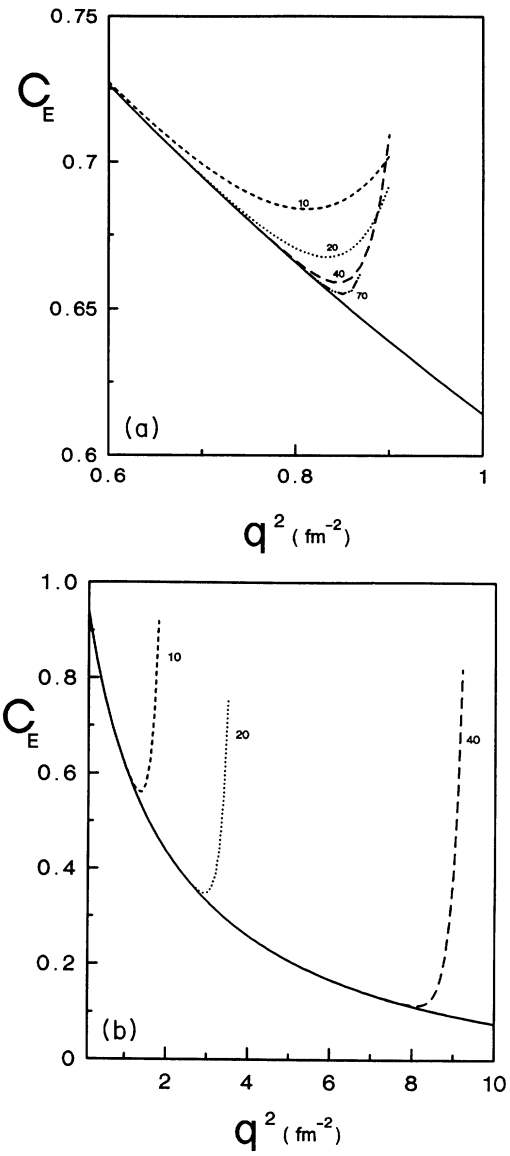

FIG. 5. The q^2 variations of the deuteron charge form factor $C_E(q^2)$ of the local potential of Table I, calculated without expanding the sine function (solid lines) and with expanding the sine function up to a certain number of terms, e.g., 10 terms (dashed lines), 20 terms (dotted lines), 40 terms (long-dashed lines), and 70 terms (dash-dotted lines). The dash-dotted line in (b) coincides with the solid line in (a). $\Delta C_E(q^2)$ is calculated analytically.

by considering the properties of the exponential integral function.

The contribution $\Delta C_E(q^2)$ to $C_E(q^2)$ is small and may be regarded as an analytic asymptotic "correction." The value of R may be chosen in the range between 12 and 16 fm. If R is large enough, e.g., $R \approx 25$ fm, $\Delta C_E(q^2)$ will be negligible. The corresponding value of $C_E(q^2)$ in this case can be used to determine the range of values of q^2 for which the determination of $\Delta C_E(q^2)$ is good. The form factor $C_E(q^2)$ was calculated twice, first by using $R \approx 25$ fm and $\Delta C_E(q^2)=0$, and second by using $R \approx 12$ fm and $\Delta C_E(q^2) \neq 0$. The two values obtained for $C_E(q^2)$ will be the same if the value of $\Delta C_E(q^2)$ is correct, for a given q^2.

The expansion of $C_E(q^2)$ in powers of q^2 at low values of q^2 is known to converge for values of q^2 below 0.9 fm^{-2} (Refs. [3,6,29]). Klarsfeld *et al.* [6] claimed that the divergence for $q^2 \geq 0.9$ fm^{-2} [see Fig. 5(a)] is caused by the Taylor's expansion of the sine function in $j_0(qr/2)=(qr/2)^{-1}\sin(qr/2)$. They used Padé approximations and the method of continued fractions to extend the q^2 range of convergence. We think that the use of the Taylor's expansion of the sine function may not cause this divergence, but it may be caused by the mutual incorporation of both of the sine expansion and the analytic forms of the radial deuteron wave functions in the formu-

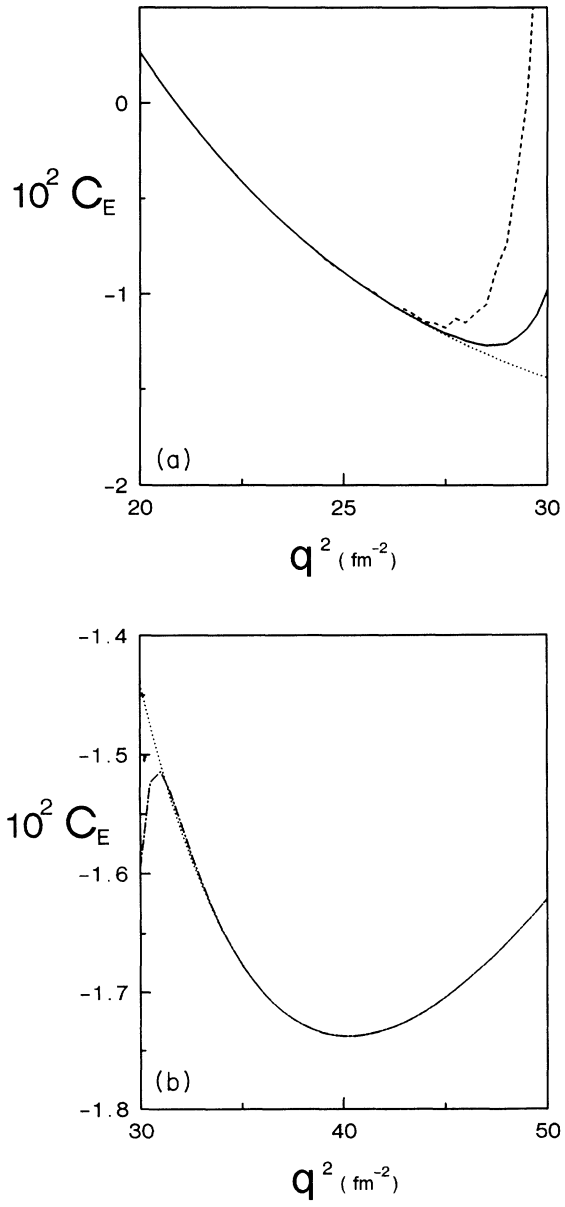

FIG. 6. The q^2 dependencies of the form factor C_E (a) obtained "independently" by using the relations (4.6) (solid line), the recurrence relations (4.8) (dashed line), and (b) the asymptotic relation (4.10) (dash-dotted line), are compared to the case of using the relation (4.1) with $R = r_C + 25$ fm (dotted line).

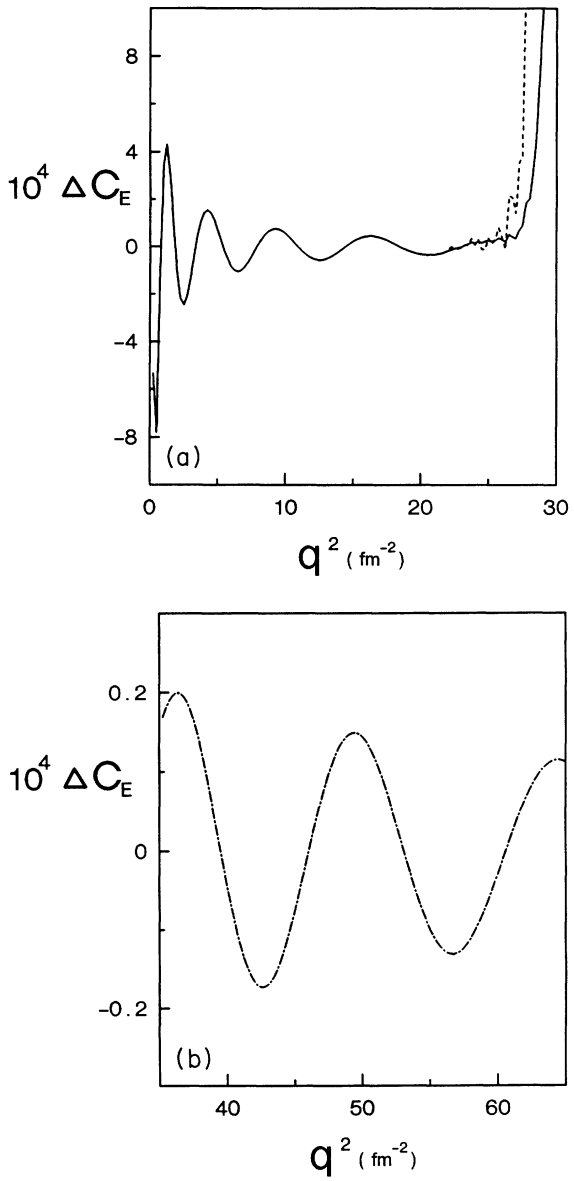

FIG. 7. The q^2 variations of the analytic asymptotic correction ΔC_E calculated by using (a) the "independent" relations (4.6) (solid lines), the recurrence relations (4.8) (dashed lines), and (b) the asymptotic relations (4.10) (dash-dotted lines).

la for $\Delta C_E(q^2)$. This may be seen from Fig. 5(b), where we show that the values of $C_E(q^2)$ given by the use of both of the Taylor's expansion of the sine function and the radial deuteron wave functions, which are obtained by *numerical* methods, converge for values of q^2 which may be relatively large, provided that enough terms are considered in the expansion.

Two new analytic formulas for $\Delta C_E(q^2)$, for which the values of $C_E(q^2)$ are correct in the ranges $0 \le q^2 \le 25$ fm^{-2} and $q^2 \ge 35$ fm^{-2}, are given below. The analytic asymptotic correction $\Delta C_E(q^2)$ is first related to the exponential integrals

$$E_n(z) = \int_1^\infty t^{-n} e^{-zt} dt \ , \tag{4.4}$$

namely,

$$\Delta C_E(q^2) = \frac{2A_S^2}{q} F_1 + \frac{2A_D^2}{q} \left[F_1 + \frac{6}{\gamma} F_2 + \frac{15}{\gamma^2} F_3 + \frac{18}{\gamma^3} F_4 + \frac{9}{\gamma^4} F_5 \right] , \tag{4.5}$$

where F_n are the imaginary parts of $E_n(z)$; then the stan-

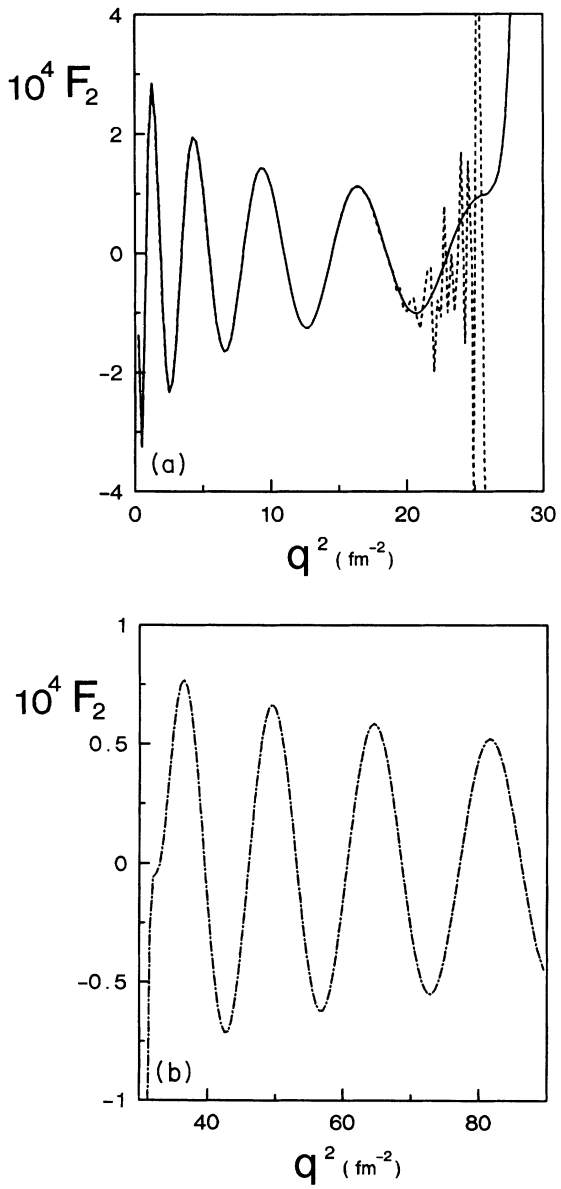

FIG. 8. The q^2 variations of F_2 obtained by using (a) the "independent" relations (4.6) (solid line), the recurrence relations (4.8) (dashed line), and by using (b) the asymptotic relation (4.10) (dash-dotted line).

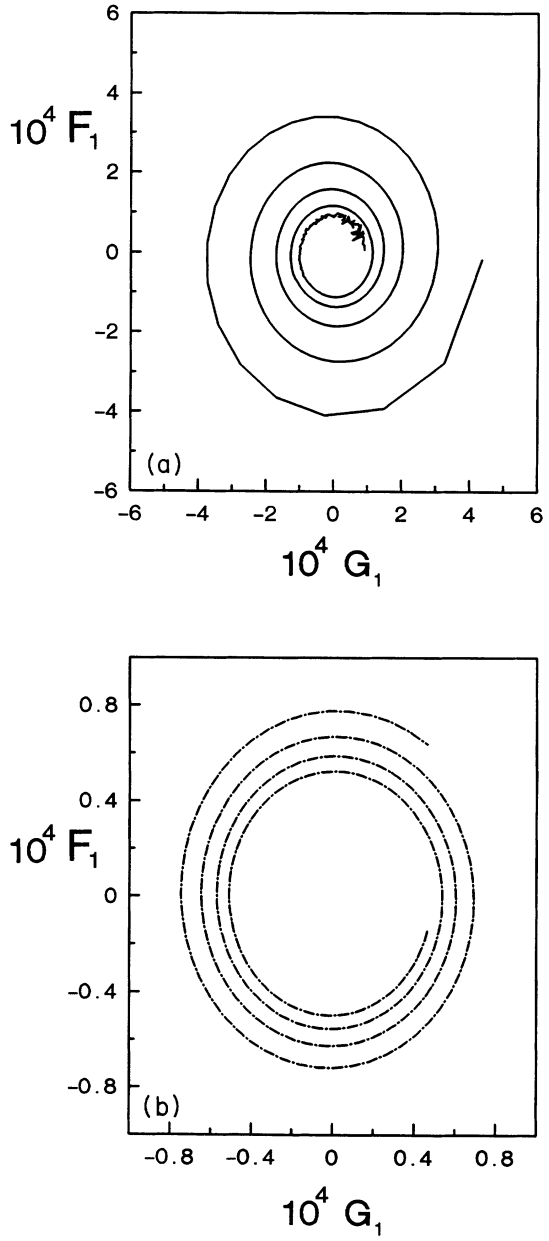

FIG. 9. The variations of G_1 versus F_1 (a) for q^2 in steps of 0.05 fm^{-2} by using the "independent" relations (4.6) in the range $0 \le q^2 \le 25$ fm^{-2} and (b) by using the asymptotic relations (4.10) in the range $35 \le q^2 \le 90$ fm^{-2} for q^2 in steps of 0.25 fm^{-2}. Larger absolute values of both of F_1 and G_1 correspond to smaller values of q^2.

dard properties of the exponential integrals [30] are used to simplify the resulting formulas.

A. Formula for $\Delta C_E(q^2)$ within the range $0<q^2\leq 25$ fm^{-2}

Accurate values of ΔC_E, in the range $0<q^2\leq 25$ fm^{-2}, may be obtained by using in Eq. (4.5) the following formulas for F_n derived from the series expansion [30] of $E_n(z)$ (see Appendix A 1 for details):

$$F_1=\vartheta+\sum_{m=1}^{m=N} a_m \sin m\vartheta \ , \tag{4.6a}$$

$$F_2=-\rho[\vartheta\cos\vartheta+(\ln\rho+\Gamma-1)\sin\vartheta]+\sum_{m=2}^{m=N} a_m \sin m\vartheta \ , \tag{4.6b}$$

$$F_3=\frac{\rho^2}{2}[\vartheta\cos 2\vartheta+(\ln\rho+\Gamma-\tfrac{3}{2})\sin 2\vartheta]+\rho\sin\vartheta+\sum_{m=3}^{m=N} a_m \sin m\vartheta \ , \tag{4.6c}$$

$$F_4=-\frac{\rho^3}{6}[\vartheta\cos 3\vartheta+(\ln\rho+\Gamma-\tfrac{11}{6})\sin 3\vartheta]+\frac{\rho}{2}\sin\vartheta-\frac{\rho^2}{2}\sin 2\vartheta+\sum_{m=4}^{m=N} a_m \sin m\vartheta \ , \tag{4.6d}$$

$$F_5=\frac{\rho^4}{24}[\vartheta\cos 4\vartheta+(\ln\rho+\Gamma-\tfrac{25}{12})\sin 4\vartheta]+\frac{\rho}{3}\sin\vartheta-\frac{\rho^2}{4}\sin 2\vartheta+\frac{\rho^3}{6}\sin 3\vartheta+\sum_{m=5}^{m=N} a_m \sin m\vartheta \ , \tag{4.6e}$$

$$z=2\gamma R-iqR/2=\rho e^{-i\vartheta}=x-iy \ ,$$

$$x=2\gamma R \ , \quad y=qR/2 \ ,$$

$$\rho=\sqrt{x^2+y^2} \ , \quad \vartheta=\tan^{-1}(q/4\gamma) \ ,$$

$\Gamma=0.577\,215\,664\,9\ldots$ is Euler's constant, and N is chosen to be 90. The coefficients a_m of the summation in F_n are given by

$$a_m=\frac{(-1)^m\rho^m}{(m-n+1)\,m!} \ , \quad m\geq n \ . \tag{4.7a}$$

For a given value of n, it is more efficient to calculate the coefficients a_m by only using both the first coefficient a_1 and the ratio a_{m+1}/a_m

$$\frac{a_{m+1}}{a_m}=-\frac{(m-n+1)\rho}{(m-n+2)(m+1)} \ , \quad m\geq n \ . \tag{4.7b}$$

The values of C_E calculated by using F_n of Eqs. (4.6) are drawn in Fig. 6(a). They are accurate to five decimal points up to $q^2\approx 25$ fm^{-2}. The variation of ΔC_E with q^2 is shown in Fig. 7(a). The imaginary parts F_n [Fig. 8(a)] change smoothly with q^2 up to $q^2\approx 22$ fm^{-2}. It is interesting that the relatively less smoother variations of F_n in the range $22\leq q^2\leq 25$ fm^{-2} do not imply incorrect values of ΔC_E and C_E within that range of q^2. The value $\Delta C_E=0$ is obtained (even for relatively small values of R) for certain values of R and q^2 because of the alternate nature of the integrand of Eqs. (4.2) and (4.5).

Alternatively, it is also possible by using the following recurrence relations to determine F_2, F_3, F_4, and F_5, and hence, $\Delta C_E(q^2)$, given that both F_1 and G_1 are known, where G_1 is the real part of $E_1(z)$:

$$F_{n+1}=\frac{1}{n}[e^{-x}\sin y+yG_n-xF_n] \ , \tag{4.8a}$$

$$G_{n+1}=\frac{1}{n}[e^{-x}\cos y-xG_n-yF_n] \ , \tag{4.8b}$$

with F_1 given in Eq. (4.6a) and G_1 from

$$G_1=-\Gamma-\ln\rho-\sum_{m=1}^{m=N} a_m\cos m\vartheta \ . \tag{4.9}$$

The coefficients a_m in (4.9) are obtained from (4.7) with $n=1$. The q^2 variations of C_E, ΔC_E, and F_n obtained by using the "recurrence" Eqs. (4.8) are compared to those obtained "directly" by using Eqs. (4.6) in Figs. 6(a), 7(a), and 8(a). The different shapes between the graphs of F_n of Eqs. (4.6) and those of Eqs. (4.8) for $q^2\gtrsim 11$ fm^{-2} do not necessarily mean obtaining different values of C_E; the values of C_E of the recurrence relations (4.8) are correct up to $q^2\approx 19$ fm^{-2}, but for $q^2>19$ fm^{-2} and again $N=90$, numerical stability is a problem: the graph representing C_E is no longer accurate, as shown in Fig. 6. We deduce that it is better to use Eqs. (4.6) than (4.8) in determining the values of the functions F_n up to $q^2=25$ fm^{-2}.

B. Formula for $\Delta C_E(q^2)$ within the range $q^2\geq 35$ fm^{-2}

For values of q^2 greater than 35 fm^{-2}, accurate values of ΔC_E and hence C_E may be obtained by using the formula for F_n obtained from the asymptotic expansion of the exponential integrals [30] $E_n(z)$ (Appendix A 2):

$$F_n=\frac{e^{-x}}{\rho}\left\{\cos y\left[\sin\vartheta-\frac{n}{\rho}\sin 2\vartheta+\frac{n(n+1)}{\rho^2}\sin 3\vartheta-\frac{n(n+1)(n+2)}{\rho^3}\sin 4\vartheta+\cdots\right]+\sin y\left[\cos\vartheta-\frac{n}{\rho}\cos 2\vartheta+\frac{n(n+1)}{\rho^2}\cos 3\vartheta-\frac{n(n+1)(n+2)}{\rho^3}\cos 4\vartheta+\cdots\right]\right\} . \tag{4.10}$$

Results of calculations for C_E, ΔC_E, F_n, and G_n which use Eqs. (4.10) are compared to those obtained by using Eqs. (4.6) and (4.8) in Figs. 6, 7, 8, and 9. The q^2 variation of C_E [Fig. 6(b)] is accurate to five decimal points for $q^2 \geq 35$ fm^{-2}. Ninety terms are summed in each of the two square brackets of Eq. (4.10).

V. INVESTIGATING THE EFFECT OF INCORPORATING AN ATTRACTIVE SHORT-RANGE NONLOCALITY IN THE *D* STATE

Mustafa and Hassan [31] and van Dijk [32] proved that it is possible to construct potentials whose scattering lengths a_t and rms radii r_D correspond to values that do not satisfy the linear a_t-r_D relation found by Klarsfeld *et al.* [6] (the a_t-r_D line does not pass through the experimental point). Potential models [33–35] incorporating short-range *repulsive* nonlocal components have relatively large values for r_D with an increase in the repulsive nonlocality strength leading to an increase in r_D (e.g., Table III in Ref. [35]). On the other hand, Kermode *et al.* [36,37] showed that an inclusion of an *attractive* short-range nonlocal component in the *S*-state radial equation will decrease r_D and hence will help in fitting simultaneously both the experimental values of r_D and a_t. This finding has also been obtained by Mustafa and Kermode [38] for a class of deuteron potential models incorporating attractive short-range tensor components that have the necessary invariance properties. The nonlocal potential presented in this section reproduces the experi-

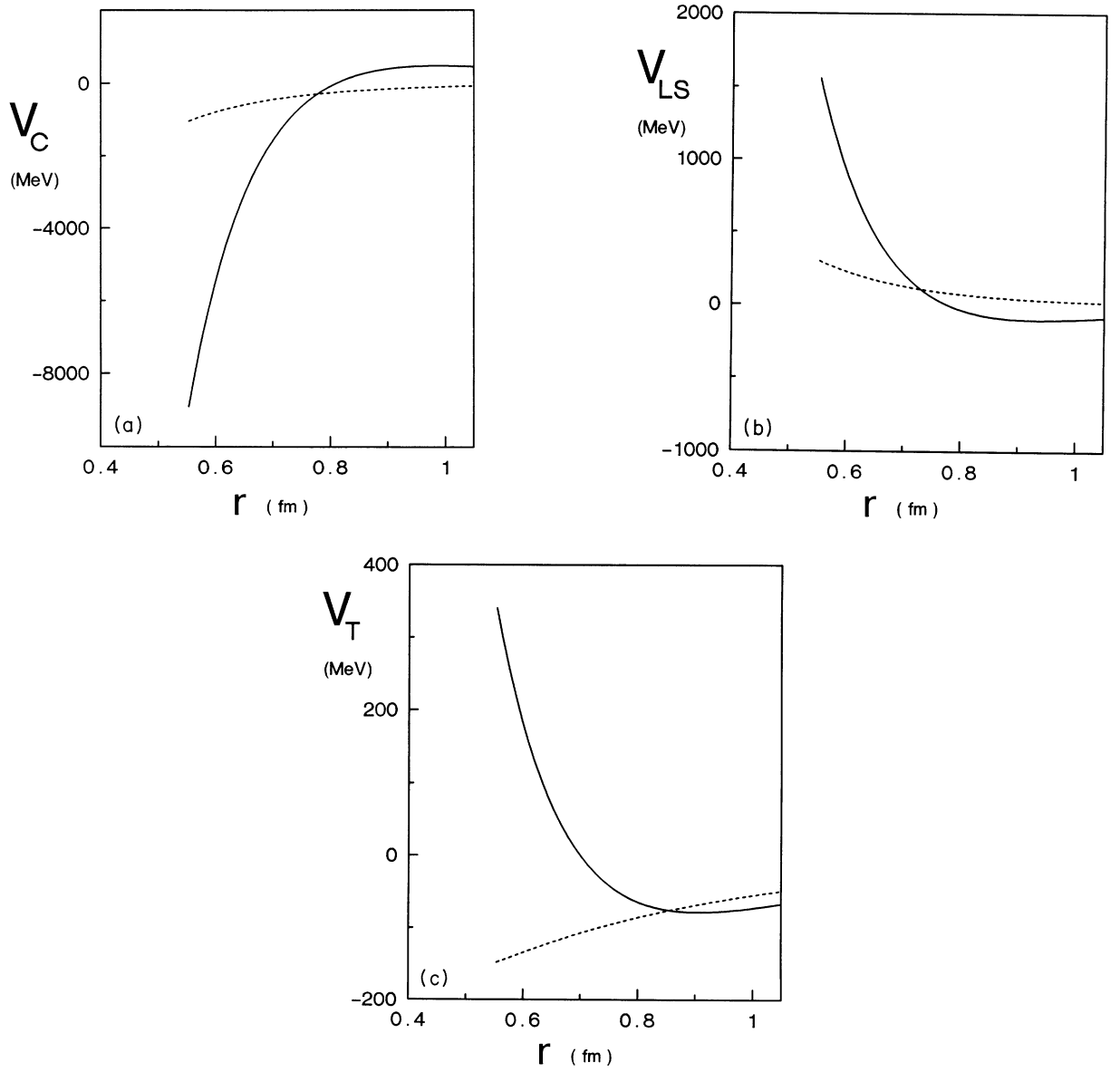

FIG. 10. (a) Central V_C, (b) spin-orbit V_{LS}, and (c) tensor V_T components of the nonlocal potential of Table IV (solid lines) are compared to the Reid hard-core potential [12] (dashed lines).

mental value of the scattering length [11] $a_t = 5.419 \pm 0.007$ fm and the new experimental value $r_D = 1.9546 \pm 0.0021$ fm of the present work.

The nonlocal potential consists of two parts–a local part $V^{(L)}$ plus a nonlocal attractive separable part $V^{(N)}$:

$$V = V^{(L)} + V^{(N)} . \tag{5.1}$$

The functional forms chosen for the local part $V^{(L)}$ are similar to those of the local potential of Table I. The coupled radial Schrödinger equations in this case have the following form:

$$\left[\frac{d^2}{dr^2} - V_C - \gamma^2\right] u(r) - 2\sqrt{2} V_T w(r) - \lambda f(r) \int_{r_c}^{\infty} f(r') u(r') dr' = 0 , \tag{5.2a}$$

$$\left[\frac{d^2}{dr^2} - \frac{6}{r^2} - V_C + 3V_{LS} + 2V_T - \gamma^2\right] w(r) - 2\sqrt{2} V_T u(r) - \lambda f(r) \int_{r_c}^{\infty} f(r') w(r') dr' = 0 , \tag{5.2b}$$

where $\lambda = -300$ fm^{-3} is the nonlocality strength, and $f(r) = e^{-\alpha r}$ with $\alpha = 2.1$ fm^{-1}. The radial dependence of the local part $V^{(L)}$ is compared to the Reid hard-core potential [12] in Fig. 10. The free parameters $A_i(n)$ are listed in Table IV.

Unlike the case of the potentials of Kermode *et al.* [36,37], where the nonlocality is only introduced in the S state, the attractive nonlocality is introduced here with equal strengths in *both* S and D channels as implied by Eqs. (5.2). No pronounced effect was found in the model value of the rms radius r_D as a result of introducing the attractive nonlocality to the D state (in addition to the S state); probably because the contribution of the w wave to r_D is much smaller than that of the u wave.

The radial deuteron wave functions u and w of this nonlocal potential are shown in Fig. 11 where they are compared with those of the Reid hard-core potential [12]. Both the u and w waves have the characteristic structures at small radii similar to those found before in the u waves by Kermode *et al.* [36,37].

VI. $C_E(q^2)$ OF THE POTENTIAL MODELS WITH SHORT-RANGE STRUCTURE IN THEIR DEUTERON WAVES

There are no special features found in the shapes of the q^2 dependences of the form factor $C_E(q^2)$ of this class of potentials, which have short-range structures in their radial deuteron wave functions. This is revealed in Fig. 12, where the q^2 dependences of the nonlocal potential of Table IV, the nonlocal potential of Kermode *et al.* [36], and the local potential of Table I are compared to that of the Reid hard-core potential [12]. It is interesting that the graphs of the form factor $C_E(q^2)$ are ordered monotonically by the "amount" of the complexity of the structure incorporated in the deuteron waves at relatively

TABLE IV. The free parameters of the nonlocal potential. $B(1) = -14.947\,142$ MeV fm and $\lambda = -300$ fm^{-3}.

n	$A_C(n)$	$A_{LS}(n)$	$A_T(n)$
1	−14.947 14	0.0	0.0
2	−2 013.984	266.5741	−442.8619
3	40 751.22	−5 228.148	5 421.484
4	−260 044.9	47 139.10	−16 591.15
5	728 816.1	−150 147.5	11 073.24
6	−680 360.6	143 155.4	7 816.735

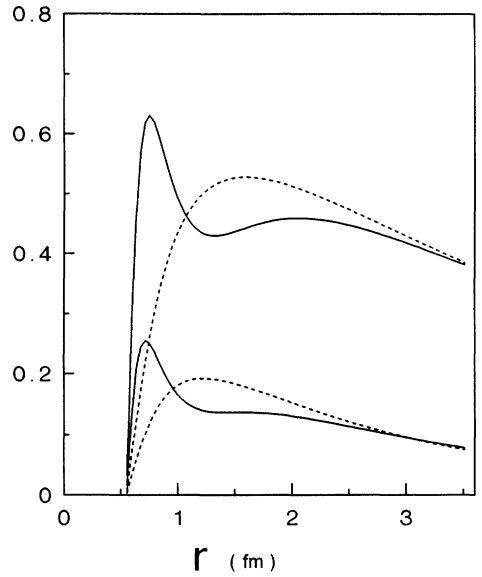

FIG. 11. The radial deuteron wave functions of the nonlocal potential of Table IV (solid lines) are compared to the Reid hard-core potential [12] (dashed lines). The upper (lower) curves are the u (w) wave functions.

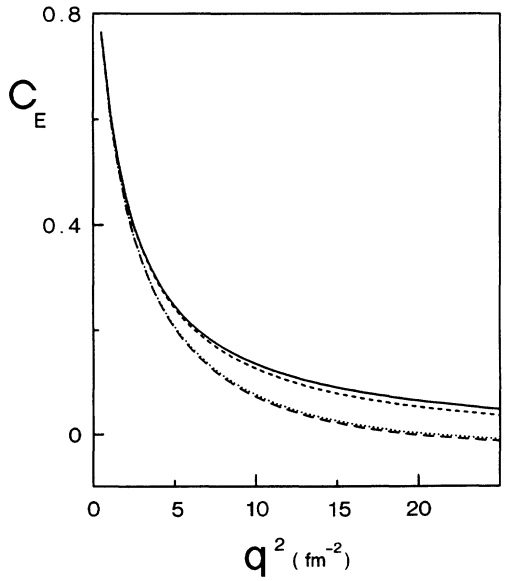

FIG. 12. The q^2 variations of the deuteron charge form factor $C_E(q^2)$ of the nonlocal potential of Table IV (solid line), the nonlocal potential of Kermode *et al.* [36] (dashed line), the local potential of Table I (dotted line), and the Reid hard-core potential [12] (long-dashed line).

small radii. The Reid hard-core potential [12], having relatively the simplest deuteron waves, is at the bottom, and the nonlocal potential of Table IV, having deuteron waves with relatively the largest complex shapes at small radii, is at the top. In between, and going upward, is the curve of the local potential of Table I, having a small "amount" of short-range structure in its w wave (Fig. 2), and the curve of the potential of Kermode *et al.* [36], having larger structure in its u wave (Fig. 3 in Ref. [36]). The existence of such correlation between the short-range structure in the deuteron waves and the magnitude of $C_E(q^2)$ is plausible since the short-range structures in the deuteron waves are associated with the non-point-like structure of the nucleon [37], and since the form factor $C_E(q^2)$ is intimately related to the deuteron structure.

ACKNOWLEDGMENTS

Support from the British Council under its Anglo-Egyptian scheme is gratefully acknowledged. M. W. K. also thanks the Physics Department of Assiut University (Sohag) for its generous hospitality.

APPENDIX: FORMULA FOR THE ANALYTIC ASYMPTOTIC CORRECTION $\Delta C_E(q^2)$

The analytic asymptotic correction $\Delta C_E(q^2)$ can be written as a sum of two parts. The first part is the u^2 part

$$\int_R^\infty u^2 \frac{\sin(qr/2)}{qr/2}dr = \frac{2A_S^2}{q}\int_R^\infty r^{-1}e^{-2\gamma r}\sin(qr/2)dr \ .$$

Putting $r=tR$ yields

$$\frac{2A_S^2}{q}\int_1^\infty t^{-1}e^{-2\gamma Rt}\sin(qRt/2)dt = \frac{2A_S^2}{q}\mathrm{Im}\int_1^\infty t^{-1}e^{-(x-iy)t}dt = \frac{2A_S^2}{q}\mathrm{Im}E_1(z) = \frac{2A_S^2}{q}F_1 \ . \tag{A1}$$

Similarly, the w^2 part of $\Delta C_E(q^2)$ can be given in terms of the imaginary parts F_n of the exponential integrals $E_n(z)$

$$\int_R^\infty w^2 \frac{\sin(qr/2)}{qr/2}dr = \frac{2A_D^2}{q}\int_R^\infty \left[1+\frac{3}{\gamma r}+\frac{3}{\gamma^2 r^2}\right]^2 e^{-2\gamma r}\frac{\sin(qr/2)}{r}dr$$

$$= \frac{2A_D^2}{q}\left[F_1+\frac{6}{\gamma}F_2+\frac{15}{\gamma^2}F_3+\frac{18}{\gamma^3}F_4+\frac{9}{\gamma^4}F_5\right] \ . \tag{A2}$$

Then, adding (A1) to (A2) gives the relation (4.5) for $\Delta C_E(q^2)$.

1. For $0 \le q^2 \le 25$ fm^{-2}

The imaginary parts F_n of the exponential integral $E_n(z)$ can be written in simple forms by using the series expansions [30] of $E_1(z)$ and $E_n(z)$:

$$E_1(z) = -\Gamma - \ln z - \sum_{m=1}^{\infty}\frac{(-1)^m z^m}{m\,m!} \tag{A3}$$

$$= -\Gamma - \ln(\rho e^{-i\vartheta}) - \sum_{m=1}^{\infty}\frac{(-1)^m \rho^m e^{-im\vartheta}}{m\,m!} \ , \tag{A4}$$

$$F_1 = \mathrm{Im}E_1(z) = \vartheta + \sum_{m=1}^{\infty}\frac{(-1)^m \rho^m \sin m\vartheta}{m\,m!} \ . \tag{A5}$$

Hence, Eq. (4.6a) for F_1 is obtained. Also, in the case of using the series expansion [30] of $E_n(z)$ for $n>1$,

$$E_n(z) = \frac{(-z)^{n-1}}{(n-1)!}(-\ln z+\psi_n) - \sum_{\substack{m=0 \\ m\neq n-1}}^{\infty}\frac{(-z)^m}{(m-n+1)\,m!}$$

$$= \frac{(-1)^{n-1}\rho^{n-1}e^{-i(n-1)\vartheta}}{(n-1)!}(-\ln\rho + i\vartheta + \psi_n) - \sum_{\substack{m=0 \\ m\neq n-1}}^{\infty}\frac{(-1)\rho^m e^{-im\vartheta}}{(m-n+1)\,m!} \ , \tag{A6}$$

where

$$\psi_1 = -\Gamma \ , \tag{A7a}$$

$$\psi_n = -\Gamma + \sum_{m=1}^{n-1}\frac{1}{m} \quad (n>1) \ . \tag{A7b}$$

Then, $F_n = \mathrm{Im}E_n(z)$

$$F_n=\frac{(-1)^{n-1}\rho^{n-1}}{(n-1)!}[\vartheta\cos(n-1)\vartheta+(\ln\rho-\psi_n)\sin(n-1)\vartheta)]-\sum_{\substack{m=0\\ m\neq n-1}}^{\infty}\frac{(-1)^m\rho^m\sin m\vartheta}{(m-n+1)\,m!}\ . \tag{A7c}$$

The formulas for F_n $(2\leq n\leq 5)$ of Eqs. (4.6) are obtained from Eqs. (A7) by the substitution with the appropriate value of n.

2. For $Q^2\geq 35$ fm^{-2}

For $q^2\geq 35$ fm^{-2}, formulas giving correct values of F_n are derived from the asymptotic expansion of $E_n(z)$ [30]:

$$E_n(z)\approx\frac{e^{-z}}{z}\left[1-\frac{n}{z}+\frac{n(n+1)}{z^2}-\frac{n(n+1)(n+2)}{z^3}+\cdots\right] \tag{A8a}$$

$$=\frac{e^{-x}}{\rho}\left[e^{i(\vartheta+y)}-\frac{n}{\rho}e^{i(2\vartheta+y)}+\frac{n(n+1)}{\rho^2}e^{i(3\vartheta+y)}-\frac{n(n+1)(n+2)}{\rho^3}e^{i(4\vartheta+y)}+\cdots\right]. \tag{A8b}$$

Then, $F_n=\mathrm{Im}E_n(z)$:

$$F_n=\frac{e^{-x}}{\rho}\left\{\cos y\left[\sin\vartheta-\frac{n}{\rho}\sin2\vartheta+\frac{n(n+1)}{\rho^2}\sin3\vartheta-\frac{n(n+1)(n+2)}{\rho^3}\sin4\vartheta+\cdots\right]\right.$$
$$\left.+\sin y\left[\cos\vartheta-\frac{n}{\rho}\cos2\vartheta+\frac{n(n+1)}{\rho^2}\cos3\vartheta-\frac{n(n+1)(n+2)}{\rho^3}\cos4\vartheta+\cdots\right]\right\} \tag{A9}$$

which is Eq. (4.10); and the real parts $G_n=\mathrm{Re}E_n(z)$:

$$G_n=\frac{e^{-x}}{\rho}\left\{\cos y\left[\cos\vartheta-\frac{n}{\rho}\cos2\vartheta+\frac{n(n+1)}{\rho^2}\cos3\vartheta-\frac{n(n+1)(n+2)}{\rho^3}\cos4\vartheta+\cdots\right]\right.$$
$$\left.-\sin y\left[\sin\vartheta-\frac{n}{\rho}\sin2\vartheta+\frac{n(n+1)}{\rho^2}\sin3\vartheta-\frac{n(n+1)(n+2)}{\rho^3}\sin4\vartheta+\cdots\right]\right\}. \tag{A10}$$

[1] R. W. Berard, F. R. Buskirk, E. B. Dally, J. N. Dyer, X. K. Maruyama, R. L. Topping, and T. J. Traverso, Phys. Lett. B **47**, 355 (1973).

[2] Yu. K. Akimov, A. N. Arvanov, G. V. Badalyan, A. E. Banifatov, D. M. Beglaryan, P. N. Bedrosyan, S. I. Bilen'kaya, K. Borcea, T. A. Vartanyan, M. A. Garzoyan, D. Dorchoman, G. G. Zograbyan, Yu. M. Kazarinov, A. L. Kalinin, V. S. Kiselev, L. I. Lapidus, G. E. Markaryan, G. I. Melikov, Ya. D. Nersesyan, O. I. Pasoyan, M. Petrascu, V. S. Pogosov, I. P. Prokhorenko, A. M. Chatrchyan, and S. A. Shatiev, Yad. Fiz. **29**, 699 (1979) [Sov. J. Nucl. Phys. **29**, 335 (1979)].

[3] G. G. Simon, Ch. Schmitt, and V. H. Walther, Nucl. Phys. **A364**, 285 (1981).

[4] L. J. Allen, J. P. McTavish, M. W. Kermode, and A. McKerrell, J. Phys. G **7**, 1367 (1981).

[5] J. P. McTavish, J. Phys. G **8**, 911 (1982).

[6] S. Klarsfeld, J. Martorell, J. A. Oteo, M. Nishimura, and D. W. L. Sprung, Nucl. Phys. **A456**, 373 (1986).

[7] V. E. Krohn and G. R. Ringo, Phys. Rev. D **8**, 1305 (1973).

[8] L. Koester, W. Nistler, and W. Waschkowski, Phys. Rev. Lett. **36**, 1021 (1976).

[9] R. Wilson, *The Nucleon-Nucleon Interaction* (Wiley, New York, 1963), Chap. 8, pp. 136–137; also, R. Wilson, in *Proceedings of the 18th International Symposium on Electron and Photon Interactions*, edited by N. B. Mistry (Cornell University Press, Ithaca, New York, 1971), pp. 98–112.

[10] M. Lacombe, B. Loiseau, R. Vinh Mau, J. Côté, P. Pirès, and R. de Tourreil, Phys. Lett. **101B**, 139 (1981).

[11] S. Klarsfeld, J. Martorell, and D. W. L. Sprung, J. Phys. G **10**, 165 (1984).

[12] R. V. Reid, Ann. Phys. (N.Y.) **50**, 411 (1968).

[13] L. Hulthén and M. Sugawara, in *Handbuch der Physik*, edited by S. Flügge (Springer-Verlag, Berlin, 1957), Vol. 39, p. 14.

[14] R. J. Adler, T. K. Das, and A. F. Filho, Phys. Rev. C **16**, 1231 (1977).

[15] V. G. J. Stoks, P. C. Van Campen, W. Spit, and J. J de Swart, Phys. Rev. Lett. **60**, 1932 (1988).

[16] I. Borbély, W. Grüebler, B. Vuaridel, and V. König, Nucl. Phys. **A503**, 349 (1989).

[17] A. R. Arndt, L. D. Roper, R. A. Bryan, R. B. Clark, B. J. VerWest, and P. Signell, Phys. Rev. D **28**, 97 (1983).

[18] R. V. Reid and L. M. Vaida, Phys. Rev. Lett. **29**, 494 (1972).

[19] D. M. Bishop and L. M. Cheung, Phys. Rev. A **20**, 381 (1979).

[20] L. J. Allen, H. Fiedeldey, and N. J. McGurk, Nucl. Phys. **4**, 353 (1978).

[21] R. de Tourreil, B. Rouben, and D. W. L. Sprung, Nucl. Phys. **A242**, 445 (1975).

[22] M. M. Mustafa, Phys. Scr. **40**, 162 (1989).

[23] R. K. Bhaduri, W. Leidemann, G. Orlandini, and E. L. Tomusiak, Phys. Rev. C **42**, 1867 (1990).

[24] D. W. L. Sprung, H. Wu, and J. Martorell, Phys. Rev. C **42**, 863 (1990).
[25] G. G. Simon, Ch. Schmitt, F. Borkowski, and V. H. Walther, Nucl. Phys. **A333**, 381 (1980).
[26] M. W. Kermode, J. R. Mines, and M. M. Mustafa, J. Phys. G **2**, L113 (1976).
[27] E. L. Lomon, Ann. Phys. (N.Y.) **125**, 309 (1980).
[28] M. Kohno, J. Phys. G **9**, L85 (1983).
[29] G. W. Erickson, Phys. Rev. Lett. **27**, 780 (1971).
[30] W. Gautschi and W. F. Cahill, in *Handbook of Mathematical Functions,* edited by M. Abramowitz and I. Stegun (Dover, New York, 1972), pp. 228–31.
[31] M. M. Mustafa and E. M. Hassan, Phys. Scr. **39**, 522 (1989).
[32] W. van Dijk, Phys. Rev. C **40**, 1437 (1989).
[33] A. McKerrell, M. W. Kermode, and M. M. Mustafa, J. Phys. G **3**, 1349 (1977).
[34] A. McKerrell, M. W. Kermode, J. R. Mines, and M. M. Mustafa, J. Phys. G **4**, 1267 (1978).
[35] M. M. Mustafa and E. S. Zahran, Phys. Rev. C **38**, 2416 (1988).
[36] M. W. Kermode, S. A. Moszkowski, M. M. Mustafa, and W. van Dijk, Phys. Rev. C **43**, 416 (1991).
[37] M. W. Kermode, W. van Dijk, D. W. L. Sprung, M. M. Mustafa, and S. A. Moszkowski, J. Phys. G **17**, 105 (1991).
[38] M. M. Mustafa and M. W. Kermode, Few Body Syst. **11**, 83 (1991).